

Access to this work was provided by the University of Maryland, Baltimore County (UMBC) ScholarWorks@UMBC digital repository on the Maryland Shared Open Access (MD-SOAR) platform.

Please provide feedback

Please support the ScholarWorks@UMBC repository by emailing scholarworks-group@umbc.edu and telling us what having access to this work means to you and why it's important to you. Thank you.

Robust implementation of quantum gates despite always-on exchange coupling in silicon double quantum dots

Utkan Güngördü* and J. P. Kestner

Department of Physics, University of Maryland Baltimore County, Baltimore, MD 21250, USA

Addressability of spin qubits in a silicon double quantum dot setup in the (1,1) charge configuration relies on having a large difference between the Zeeman splittings of the electrons. When the difference is not sufficiently large, the rotating wave approximation becomes inaccurate. We consider a device working in this regime, with always-on exchange coupling, and describe how a CZ gate and arbitrary one-qubit gates which are robust against charge noise can be implemented by smoothly pulsing the microwave source, while eliminating the crosstalk stroboscopically. We find that the most significant deviations from the rotating wave approximation, which are analogous to the Bloch-Siegert shift in a two-level system, can be compensated using local virtual gates.

I. INTRODUCTION

Silicon is a promising platform for practical quantum computing. Fidelities nearing 99.99% have recently been reported for one-qubit gates in Si/SiGe [1] and above 99.9% in SiMOS and Si/SiO₂ [2, 3]. However, a universal quantum computer requires entangling operations as well [4], and the infidelities for two-qubit gates remain orders of magnitude higher [5–9]. Hyperfine coupling with remnant spinful isotopes such as ²⁹Si and ³⁰Si is one source of errors, but the concentration of these isotopes can be reduced down to 800ppm [1, 3, 10] or lower [11], essentially eliminating it as a concern. Another significant source of errors is charge noise, which remains a problem [12–17]. Although it can be partially mitigated when operating at a “sweet spot” where the exchange is insensitive to the leading order effects of the electrostatic fluctuations in gate voltages [8], even there the second order fluctuations can still be large, and there can be fluctuations in the tunnel barrier as well [18]. Thus, schemes to correct charge noise are of great importance for scalable quantum computation in semiconductor devices.

Quantum dot setups in which the spin of each electron is treated as a qubit are particularly attractive. Typical implementations of one-qubit gates require the ability to address one of the qubits without affecting the other one. In setups using electron dipole spin resonance (EDSR) [7, 8], this is done by placing a micromagnet such that one of the electrons is closer to the micromagnet than the other one, providing a strong magnetic field gradient. The resulting difference between the Zeeman energy splittings of the electrons, δE_z , separates their resonant frequencies and allows implementation of fast [19, 20] or dynamically corrected [21] two-qubit gates to suppress the impact of the charge noise on the exchange. However, the micromagnet can also couple charge noise directly to the spins through the effective spin-orbit interaction, opening a new way for gate errors to enter. In setups with electron spin resonance (ESR) [6, 10], on

the other hand, the spins remain largely isolated from the electrical environment in the absence of coupling. A difference in resonant frequencies then comes only via a difference in the g -factors of the electrons. The effective g -factors of the electrons strongly depend on the interface hosting the 2DEG [22–24], which is an aspect of the fabrication that cannot be controlled perfectly, and although the resulting δE_z can be electrically [16] or magnetically [25] tunable to a certain extent, the maximum accessible value is typically much less than that provided by a micromagnet [7]. In a double quantum dot setup, this causes two issues with addressability. First, addressability is diminished due to the failure of the rotating wave approximation.

Second, when the exchange interaction is turned on, this further leads to exchange-induced crosstalk between the two electrons.

In Ref. [21], we described a robust pulse sequence which implements a CZ gate in silicon double quantum dots while correcting charge noise. However, this scheme relies on having access to high-fidelity one-qubit gates in the (1,1) charge region while also having fully controllable exchange coupling. In devices where addressability is poor, or where exchange cannot be turned off [10], implementation of high-fidelity one-qubit gates is difficult, even in the absence of any stochastic errors such as charge noise.

In this paper, we simultaneously solve both issues of charge noise and addressability in the presence of an always-on exchange coupling and small δE_z by deriving shaped pulses that implement a robust CZ gate, as well as robust, arbitrary one-qubit gates.

This paper is organized as follows. In Section II, we describe the effective Hamiltonian for the silicon double quantum dot in the (1,1) charge region, and discuss how it algebraically splits into a pair of independent two-level systems when the rotating wave approximation holds. In Section III, we show that although errors from the rotating wave approximation are significant, they can be compensated for by using only local Z rotations. In Section IV, we show how the results from Ref. [26] can be used to suppress charge noise in the two-qubit system, followed by Section V where we explicitly construct ro-

* utkan@umbc.edu

bust CZ and robust arbitrary one-qubit gates. Section VI concludes the paper.

II. MODEL

Electrons in a double quantum dot in the (1,1) charge region in the far detuning regime ($U + \epsilon \ll U - \epsilon$) can be modeled by the following Hamiltonian [27, 28]

$$H = \begin{pmatrix} \bar{E}_z & \frac{E_{2,\perp}^*}{2} & \frac{E_{1,\perp}^*}{2} & 0 & 0 \\ \frac{E_{2,\perp}}{2} & \frac{\delta E_z}{2} & 0 & \frac{E_{1,\perp}}{2} & t_0 \\ \frac{E_{1,\perp}}{2} & 0 & -\frac{\delta E_z}{2} & \frac{E_{2,\perp}}{2} & -t_0 \\ 0 & \frac{E_{1,\perp}}{2} & \frac{E_{2,\perp}}{2} & -\bar{E}_z & 0 \\ 0 & t_0 & -t_0 & 0 & U - \epsilon \end{pmatrix} \quad (1)$$

in the basis of $|\uparrow\uparrow\rangle, |\uparrow\downarrow\rangle, |\downarrow\uparrow\rangle, |\downarrow\downarrow\rangle, |S(0,2)\rangle$, which includes the possibility of tunneling of one of the electrons to its neighboring dot and occupying the singlet state $|S(0,2)\rangle$. The energy of the $|S(2,0)\rangle$ is too large in this setup and thus neglected. Above, $\bar{E}_z = \mu_B(g_1 B_z^1 + g_2 B_z^2)/2$ and $\delta E_z = \mu_B(g_1 B_z^1 - g_2 B_z^2)$ denote the average and difference in Zeeman energies of the electrons due a magnetic field provided by an external static magnet, t_0 is tunneling energy, E_{\perp}^k is the Zeeman energy $\mu_B g_k (B_x^k + i B_y^k)$ due to oscillating microwave source as seen by the k th electron, $U \mp \epsilon$ is the on-site electrostatic energy where ϵ is the detuning from the applied gate voltage through. We will express E_{\perp}^k as $\Omega_k e^{i\omega t}$ where Ω_k is the slowly varying (compared to the timescale $1/\omega$) microwave amplitude and ω is the microwave frequency,

such that

$$\Omega_k e^{i\omega t} = \mu_B g_k (B_x^k + i B_y^k). \quad (2)$$

In the typical experimental regime of $U - \epsilon \gg t_0, \delta E_z$, one can use Schrieffer-Wolff transformation to block-diagonalize H and obtain the following spin Hamiltonian [19, 21]

$$H \approx \begin{pmatrix} \bar{E}_z & \frac{E_{2,\perp}^*}{2} & \frac{E_{1,\perp}^*}{2} & 0 \\ \frac{E_{2,\perp}}{2} & \frac{\delta E_z}{2} - \frac{J}{2} & \frac{J}{2} & \frac{E_{1,\perp}^*}{2} \\ \frac{E_{1,\perp}}{2} & \frac{J}{2} & -\frac{\delta E_z}{2} - \frac{J}{2} & \frac{E_{2,\perp}^*}{2} \\ 0 & \frac{E_{1,\perp}}{2} & \frac{E_{2,\perp}}{2} & -\bar{E}_z \end{pmatrix}, \quad (3)$$

where $J \equiv 2t_0^2/U - \epsilon$ is the tunneling mediated exchange coupling between the two electrons. This Heisenberg-type exchange coupling mixes $|\uparrow\downarrow\rangle$ and $|\downarrow\uparrow\rangle$ states; however, when it is changed slowly ($\dot{J} \ll \delta E_z/\hbar$ when assuming $J \ll \delta E_z$ [21]) or held fixed (as is the case we will focus on), one can instead work in the eigenbasis of the Hamiltonian (at $\Omega_i = 0$), in which all states become decoupled and the exchange coupling becomes Ising-like [19, 21, 29]. To this end, let us denote the four eigenvectors of $H|_{\Omega_i=0}$ as $|\uparrow\uparrow\rangle, |\psi_+(t)\rangle, |\psi_-(t)\rangle, |\downarrow\downarrow\rangle$. We then transform to the logical basis of $\{e^{i\phi_{\uparrow\uparrow}(t)}|\uparrow\uparrow\rangle, e^{i\phi_+(t)}|\psi_+(t)\rangle, e^{i\phi_-(t)}|\psi_-(t)\rangle, e^{i\phi_{\downarrow\downarrow}(t)}|\downarrow\downarrow\rangle\}$ using $H_R = R^\dagger H R + i\hbar(\partial_t R^\dagger)R$, where R is the transformation matrix whose rows are given by the logical basis states and $\phi_i(t)$ are yet undetermined degrees of freedom, associated with shifts in ZZ, IZ, ZI terms in the Hamiltonian in this new frame. We thus obtain the rotating frame Hamiltonian

$$H_R = \begin{pmatrix} \bar{E}_z + \dot{\phi}_{\uparrow\uparrow} & \frac{(\bar{E}_{2,\perp}^+)^*}{2} e^{-i(\phi_{\uparrow\uparrow} - \phi_+)} & \frac{(\bar{E}_{1,\perp}^+)^*}{2} e^{-i(\phi_{\uparrow\uparrow} - \phi_-)} & 0 \\ \frac{\bar{E}_{2,\perp}^+}{2} e^{i(\phi_{\uparrow\uparrow} - \phi_+)} & \frac{1}{2}(-J + \Delta E) + \dot{\phi}_+ & \tilde{V} & \frac{(\bar{E}_{1,\perp}^-)^*}{2} e^{i(\phi_{\downarrow\downarrow} - \phi_+)} \\ \frac{\bar{E}_{1,\perp}^+}{2} e^{i(\phi_{\uparrow\uparrow} - \phi_-)} & \tilde{V}^* & \frac{1}{2}(-J - \Delta E) + \dot{\phi}_- & \frac{(\bar{E}_{2,\perp}^-)^*}{2} e^{i(\phi_{\downarrow\downarrow} - \phi_-)} \\ 0 & \frac{\bar{E}_{1,\perp}^-}{2} e^{-i(\phi_{\downarrow\downarrow} - \phi_+)} & \frac{\bar{E}_{2,\perp}^-}{2} e^{-i(\phi_{\downarrow\downarrow} - \phi_-)} & -\bar{E}_z + \dot{\phi}_{\downarrow\downarrow} \end{pmatrix} \quad (4)$$

where $\Delta E = \sqrt{\delta E_z^2 + J^2}$ is the energy splitting between the adiabatic eigenstates of H with zero net spin, \tilde{V} is a diabatic correction which vanishes when J and δE_z do not vary in time [21]. The transverse terms in the logical adiabatic basis are given by [21]

$$\begin{aligned} \tilde{E}_{1,\perp}^\pm &= \tilde{\Omega}_1^\pm e^{i\omega t} = \frac{(\Delta E + \delta E_z)\Omega_1 \mp J\Omega_2}{\sqrt{2\Delta E(\Delta E + \delta E_z)}} e^{i\omega t}, \\ \tilde{E}_{2,\perp}^\pm &= \tilde{\Omega}_2^\pm e^{i\omega t} = \frac{(\Delta E + \delta E_z)\Omega_2 \pm J\Omega_1}{\sqrt{2\Delta E(\Delta E + \delta E_z)}} e^{i\omega t}. \end{aligned} \quad (5)$$

This exchange-induced mixing of one-qubit ‘‘Rabi frequencies’’, which we recognize as a form of crosstalk, is

a result (and the cost) of working in the adiabatic basis with the simplified Ising-type exchange coupling. We proceed by fixing the gauge with the choice $\dot{\phi}_\pm = \mp \Delta E/2$ and $\dot{\phi}_{\uparrow\uparrow} = \dot{\phi}_{\downarrow\downarrow} = -\bar{E}_z$, and tune the microwave frequency to $\hbar\omega = \bar{E}_z - \Delta E/2$ such that if the rotating wave approximation held and the ‘‘fast’’ oscillating terms were negligible, we would have addressed only the second qubit (we can similarly tune into the first qubit by tuning the microwave as $\hbar\omega = \bar{E}_z + \Delta E/2$). This leads to the Hamil-

tonian

$$H_R = \begin{pmatrix} 0 & \frac{\tilde{\Omega}_2^+}{2} & \frac{\tilde{\Omega}_1^+}{2} e^{\frac{i}{\hbar} \Delta E t} & 0 \\ \frac{\tilde{\Omega}_2^+}{2} & -\frac{J}{2} & 0 & \frac{\tilde{\Omega}_1^-}{2} e^{\frac{i}{\hbar} \Delta E t} \\ \frac{\tilde{\Omega}_1^+}{2} e^{-\frac{i}{\hbar} \Delta E t} & 0 & -\frac{J}{2} & \frac{\tilde{\Omega}_2^-}{2} \\ 0 & \frac{\tilde{\Omega}_1^-}{2} e^{-\frac{i}{\hbar} \Delta E t} & \frac{\tilde{\Omega}_2^-}{2} & 0 \end{pmatrix}. \quad (6)$$

We note in passing that we will consider modulation of the envelope function Ω_i as a function of time as well in what follows, but these modulations will be much slower than ω , so this decomposition of the microwave field into amplitude and frequency is still meaningful.

In the experiments in Refs. [7, 8], δE_z is provided by an on-chip micromagnet which results in a strong magnetic field gradient, and a δE_z that is much larger than Ω_2 . However, in the setups of Refs. [2, 10], δE_z is due to the differences between g -factors (which can be modulated by the gate voltages [16] or by changing the orientation of the external magnet [25]), and leads to a smaller $\delta E_z \sim 10$ MHz, in which case the rotating wave approximation no longer holds.

Charge noise causes fluctuations in the exchange coupling $J \rightarrow \tilde{J} = J + \delta J$. Furthermore, spinful isotopes cause stochastic fluctuations in Zeeman splittings, ϵ_1 and ϵ_2 , through hyperfine coupling, although this can be remedied by using a purified silicon with lower concentration of spinful silicon isotopes [11].

With these sources of errors in mind, we can write the overall Hamiltonian as the sum of a noisy control and an oscillatory term, $\tilde{H}_R = \tilde{H}_c + H_{\text{osc}}$ where

$$\begin{aligned} \tilde{H}_c &= \frac{\gamma \Omega_2}{2} IX + \frac{\gamma \Omega_1}{2} \eta ZX + \frac{\tilde{J}}{4} ZZ + \epsilon_1 ZI + \epsilon_2 IZ, \\ H_{\text{osc}} &= \frac{\gamma \Omega_1}{2} [XI \cos(\Delta E t) + YI \sin(\Delta E t)] + \\ &\quad \frac{\eta \Omega_2}{2} [XZ \cos(\Delta E t) + YZ \sin(\Delta E t)] \end{aligned} \quad (7)$$

and

$$\gamma = \frac{(\Delta E + \delta E_z)}{\sqrt{2\Delta E(\Delta E + \delta E_z)}}, \quad \eta = \frac{J}{\sqrt{2\Delta E(\Delta E + \delta E_z)}}. \quad (8)$$

We will limit ourselves to exchange strengths smaller than the difference in Zeeman splittings, such that $J/\delta E_z$, despite being non-negligible, can nevertheless be treated as smallness parameter allowing a perturbative treatment. Then, to the leading order in $J/\delta E_z$, $\gamma \approx 1$ and $\eta \approx J/2\delta E_z$. Moreover, we can neglect the perturbations in γ and η due to exchange noise, because the δJ terms are suppressed by the smallness factor of $J/\delta E_z^2$ and we limit ourselves to $J \ll \delta E_z$. Exchange noise in ΔE can also be neglected where it is suppressed by the smallness factor $J/\delta E_z$.

At this point, we note that the control Hamiltonian H_c fits into the embedding $\mathfrak{su}(2) \oplus \mathfrak{su}(2) \oplus \mathfrak{u}(1) \subset \mathfrak{su}(4)$.

The generators of these commuting $\mathfrak{su}(2)$ algebras are $X_{\pm}, Y_{\pm}, Z_{\pm} \equiv \{(IZ \pm ZZ)/2, -(IY \pm ZY)/2, (IX \pm ZX)/2\}$ and the $\mathfrak{u}(1)$ is generated by $Q \equiv ZI$. Explicitly, H_c can be split into three commuting parts

$$H_c = H_+ + H_- + H_q \quad (9)$$

where

$$\begin{aligned} H_{\pm} &\equiv \Omega_{\pm} X_{\pm} + \beta_{\pm} Z_{\pm} & H_q &\equiv \epsilon_1 ZI \\ \Omega_{\pm} &\equiv \frac{\gamma \Omega_2}{2} \left(1 \pm \frac{1}{\gamma} \frac{g_1}{g_2} \eta \right), & \tilde{\beta}_{\pm} &\equiv \epsilon_2 \pm \frac{\tilde{J}}{4}, \end{aligned} \quad (10)$$

where we used Eq. (2) to express Ω_1 as $\Omega_2 g_1/g_2$.

III. BLOCH-SIEGERT SHIFT FOR THE TWO-QUBIT SYSTEM

In this section, we will apply the rotating wave approximation and also show how to compensate for the leading order corrections to the approximation, and in the following section, we will show how one can obtain a shaped pulse $\Omega_2(t)$ which can suppress the leading order effect of the terms δJ , ϵ_2 and η from the final time evolution operator $U(t_f)$.

The validity of the rotating wave approximation hinges on the value of $\delta E_z/\hbar$. This value is 1.3 GHz in the Si/SiGe device from Ref. [7] and 210 MHz in the Si/SiGe device from Ref. [8], both of which incorporate micromagnets and operate via EDSR. However, in the Si/SiO₂ device from Ref. [3, 10], operating via ESR, this value is limited to around 15 MHz, for which the rotating wave approximation to neglect H_{osc} fails, resulting in poor gate fidelities. In this section, we will show that the most significant contribution from the oscillatory terms can nevertheless be easily compensated.

To this end, we treat H_{osc} as an interaction Hamiltonian and obtain the total time evolution operator as a product of the time evolution operators due to H_c and H_{osc} as

$$U_{\text{total}} = U_c(t_f; -t_f) U_{\text{osc}}(t_f; -t_f) \quad (11)$$

where $U_{\text{osc}}(t; -t_f)$ is the solution to the Schrödinger equation

$$\begin{aligned} i\dot{U}_{\text{osc}}(t; -t_f) &= \bar{H}_{\text{osc}}(t) U_{\text{osc}}(t; -t_f) \\ \bar{H}_{\text{osc}} &\equiv U_c^\dagger(t; -t_f) H_{\text{osc}}(t) U_c(t; -t_f) \end{aligned} \quad (12)$$

When ΔE is larger than the microwave amplitude, one can obtain U_{osc} in a perturbative manner using Magnus expansion

$$U_{\text{osc}}(t; -t_f) = e^{\sum_{n=1}^{\infty} \Phi_n}, \quad (13)$$

This allows use to obtain corrections to the rotating wave approximation perturbatively in powers of the smallness

factor $\Omega_2(t)/\Delta E$, as will be made clear shortly. The first order term in the Magnus expansion

$$\Phi_1 = -\frac{i}{\hbar} \int_{t_0}^{t_f} dt' \bar{H}_{\text{osc}}(t') \quad (14)$$

is negligible when $\Delta E \gg \pi/t_f$. For example, for a gate time $t_f \sim 10\mu\text{s}$, we find that a value of $\Delta E \sim 10\text{MHz}$, which is readily attainable in experiments, is sufficiently large.

The leading order correction, then, is

$$\Phi_2 = -\frac{1}{2\hbar^2} \int_{t_0}^{t_f} dt' \int_{t_0}^{t'} dt'' [\bar{H}_{\text{osc}}(t'), \bar{H}_{\text{osc}}(t'')]. \quad (15)$$

We now show how this can be reduced to a simple condition with good accuracy.

The first simplification we make is to note that in H_{osc} , given explicitly in Eq. (7), the contribution of η is suppressed by the smallness factor $J/\Delta E$ compared to γ . Thus, we neglect the terms proportional to η . The “fast” oscillations in H_{osc} can be eliminated by (temporarily) going into a rotating frame defined by the transformation $S = e^{i\Delta E t Z I}$, which leads to

$$H_{\text{osc}}^S = \frac{\gamma\Omega_2(t)}{2} X I + \Delta E Z I \quad (16)$$

Since $S \in \text{U}(1)$ commutes with $U(t; t_0) \in \text{SU}(2) \times \text{SU}(2)$, we can change the ordering of these transformations, and obtain

$$U_{\text{osc}}(t; t_0) = e^{\frac{i}{\hbar} \Delta E t Z I} \mathcal{T} e^{-\frac{i}{\hbar} \int dt U_c^\dagger(t; t_0) H_{\text{osc}}^S(t) U_c(t; t_0)}, \quad (17)$$

back in the frame of Eq. (7). Although we can use second order Magnus expansion given by Φ_2 as is to approximately evaluate the time-ordered integration above at this point, we instead notice that ZI term in the integrand above commutes with $U(t; t_0)$, and the weak (when compared to ΔE) term $\gamma\Omega_2(t)U^\dagger(t; t_0)[XI]U(t; t_0)/2$ anticommutes with ZI at all times, forming a dynamical $\mathfrak{su}(2)$ algebra. Based on this, we approximate the leading order correction Φ_2 by an averaged Bloch-Siegert shift and obtain:

$$U_{\text{osc}}(t_f; t_0) \approx \exp \left[-i \frac{1}{\hbar \Delta E} \int_{t_0}^{t_f} dt \left(\frac{\gamma\Omega_2(t)}{2} \right)^2 ZI \right]. \quad (18)$$

The inverse of this rotation can then be applied prior to the actual gate U_{total} (cf. Eq. (11)) to compensate for the unwanted ZI Bloch-Siegert rotation.

An alternative way of obtaining this correction would be to solve the Schrödinger equation Eq. (12) numerically. U_{osc} tends to be a rotation mostly around ZI , so we can pick up the ZI part of this $\text{SU}(4)$ rotation, which can be corrected for easily, using

$$U_{\text{osc}}^{(ZI)} = e^{i\Theta ZI}, \quad \Theta \equiv \text{tr}(-i \ln[U_{\text{osc}}(t_f; -t_f)] ZI).$$

We numerically find that the approximations we made in this section lead to deviations in trace gate fidelity which depend on $\Omega_2(t)/\Delta E$, and can be as small as $\sim 10^{-4}$ with a suitable and experimentally attainable choice when using the parameters from Refs. [3, 10]. The numerical results for each gate are given in Section V.

Overall, the results from this section allow us to easily compensate for the shortcomings of the rotating wave approximation by applying a (virtual [30–32]) ZI rotation given in Eq.(18) to undo $U_{\text{osc}}(t_f; t_0)$ in Eq. (11). This compensation can be done before, after or during the gate; the ordering does not matter because ZI is the $\mathfrak{u}(1)$ and commutes with the control Hamiltonian. We thus need not carry H_{osc} forward in what follows, as it is now compensated for separately.

IV. ROBUST GATES

In this section, we briefly summarize the results from [26], and show how they can be adapted to the double quantum dot system. In the next section, we will present specific applications for obtaining a robust CZ gate and robust, arbitrary one-qubit gates.

Consider a time evolution from $t = 0$ to t_f of a two-level system described by the noisy Hamiltonian

$$H(t) = [\Omega(t) + g(t)\epsilon_Z]Z + [\beta + \epsilon_X]X. \quad (19)$$

where ϵ_Z and ϵ_X are quasistatic, stochastic noise terms. The leading order effects of these noise terms from the time evolution at the final time t_f can be eliminated if $\Omega(t)$ is a shaped pulsed obtained from a function $\Phi(\chi(t))$, through the following relation

$$\Omega(t) = \bar{\Omega}(\chi) \equiv -\beta \sin(2\chi) \times \frac{\Phi''(\chi) + 4\Phi'(\chi) \cot(2\chi) + [\Phi'(\chi)]^3 \sin(4\chi)}{2\sqrt{1 + [\Phi'(\chi) \sin(2\chi)]^2}} \quad (20)$$

where $\chi = \chi(t)$ is a reparametrization of time determined by $\Phi(\chi)$ through the relation

$$\beta t = \hbar \int_0^{\chi_f} d\chi \sqrt{1 + [\Phi'(\chi) \sin(2\chi)]^2}, \quad (21)$$

$\Phi(\chi(t))$ is any function which obeys the constraints [26]

$$\sin(4\chi_f) + 8e^{-2i\Phi(\chi_f)} \int_0^{\chi_f} d\chi \sin^2(2\chi) e^{2i\Phi(\chi_f)} \int_0^{\chi_f} = 0, \quad (22a)$$

$$\int_0^{\chi_f} \sin^2(2\chi) \Phi'(\chi) = 0, \quad (22b)$$

$$\int_0^{\chi_f} d\chi \sin(2\chi) \bar{g}(\chi) e^{2i\Phi(\chi_f)} \sqrt{1 + [\Phi'(\chi) \sin(2\chi)]^2} = 0 \quad (22c)$$

$$\int_0^{\chi_f} d\chi \cos(2\chi) \bar{g}(\chi) \sqrt{1 + [\Phi'(\chi) \sin(2\chi)]^2} = 0, \quad (22d)$$

and $\bar{g}(\chi) \equiv g(t)$. The function $\Phi(\chi)$ must satisfy the following initial conditions

$$\Phi(0) = 0, \quad \Phi'(0) = 0 \quad (23)$$

to ensure that the initial time evolution operator is the identity. The resulting gate $U(t_f; 0)$ is determined by the values of $\Phi(\chi_f)$ and $\Phi'(\chi_f)$ [26].

We focus on the particular case of $g(t) = \Omega(t)$ (i.e., multiplicative noise in the control field), or equivalently, $\bar{g}(\chi) = \Omega(\chi)$. If $\Phi'(\chi)$ is an odd function of χ (which itself is an odd function of t), the pulse shape $\Omega(\chi)$ becomes an odd function of time as well. Since this means the integrand of robustness conditions Eqs. (22b) and (22d) are odd functions for time, we can consider expanding the time evolution to the symmetric interval from $t = -t_f$ to $t = t_f$, which ensures that the integrals vanish and both conditions are satisfied [26]. When the system is pulsed from $t = t_0 = -t_f$ to $t = t_f$ using a pulse that is odd in time, the resulting time evolution is given by [26, 33]

$$U(t_f; -t_f) = Z_\phi X_\theta Z_{-\phi} = e^{-i\frac{\theta}{2}(\cos\phi X + \sin\phi Y)}, \quad (24)$$

$$\phi \equiv \text{sgn}[\Phi'(\chi_f)] \arccos \sqrt{1 + [\Phi'(\chi_f) \sin(2\chi_f)]^2}, \quad \theta \equiv 4\chi_f,$$

where X_θ is a θ rotation around the X axis and Z_ϕ is defined similarly. We refer to the Supplementary Information in Ref. [26] for the lengthy derivation of these results.

We now show how these results can be used to suppress the effects of δJ and η in \hat{H}_c from the final time evolution operator $U(t_f)$ in the double quantum dot system [34]. Although the four-level problem is algebraically split into a commuting pair of two-level systems and a single-level system, or $\mathfrak{su}(2) \oplus \mathfrak{su}(2) \oplus \mathfrak{u}(1)$, we see from Eq. (10) that the dynamics of these $\mathfrak{su}(2)$ s are completely dependent: that is, choosing the pulse shape $\Omega_\pm(t)$ and the (time-independent) “energy splitting” β_\pm for one $\mathfrak{su}(2)$ fixes the values $\Omega_\mp(t)$ for the other $\mathfrak{su}(2)$. This means that additional care is required when choosing suitable generating functions $\Phi_\pm(\chi)$ for each $\mathfrak{su}(2)$, and that $\Phi_+(\chi)$ and $\Phi_-(\chi)$ cannot be chosen independently—in fact, choosing one completely determines the other.

We now show that even under this constraint, we can still use the results from Ref. [26] to implement a robust quantum gate in the four-level system when the exchange is held fixed and the microwave source is smoothly pulsed in time.

First, from Eq. (10), we observe that in the absence of the stochastic noise and η terms, we have

$$\beta_+ = -\beta_-, \quad \Omega_+(t) = \Omega_-(t). \quad (25)$$

Keeping Eq. (20) in mind, we realize that the choice

$$\Phi_-(\chi) = -\Phi_+(\chi) \quad (26)$$

would be compatible with these dynamical constraints between the $\mathfrak{su}(2)$ subsystems. We are thus treating the entire $\eta\Omega_2(t)ZXg_1/2\gamma g_2$ term as “noise”, and not just the (already neglected) truly stochastic part which is due to δJ ; this assumption is not strictly necessary, but it is convenient as it allows us to establish a very simple relationship between the two generating functions $\Phi_-(\chi)$ and $\Phi_+(\chi)$.

With this choice, the overall robust time evolution for the four-level system can thus be obtained as

$$\mathcal{R}(\theta, \phi) \equiv \mathcal{R}_+(\theta, \phi) \mathcal{R}_-(\theta, \phi),$$

$$\mathcal{R}_\pm(\theta, \phi) \equiv Z_\pm(\phi) X_\pm(\pm\theta) Z_\pm(-\phi), \quad (27)$$

where \mathcal{R}_\pm denotes the time evolution for each $\mathfrak{su}(2)$ subsystem. The rotation angle θ has alternating signs because $\beta_+ = -\beta_-$, corresponding to time-inversion following Eq. (21), which implies a sign flip in the overall rotation angle in Eq. (24). Combining similar commuting terms, this simplifies to

$$\mathcal{R}(\theta, \phi) = IX_\phi ZZ_\theta IX_{-\phi} \quad (28)$$

The pulse for the opposite sign, $\phi \rightarrow -\phi$, can be obtained by the replacement $\Phi(\chi) \rightarrow -\Phi(\chi)$ which implies $\Omega(t) \rightarrow -\Omega(t)$, following respectively from Eqns. (24) and (20). We will use this expression when targeting specific gates in the next section.

V. EXAMPLES OF ROBUST GATES

For obtaining numerical results when targeting specific gates in this section, we will use the following ansatz:

$$\Phi_+(\chi) = a_1 \chi^2 + \text{sgn}(\chi) \left[a_2 \chi^3 + \sum_{i=1}^8 b_i \sin(n\pi\chi/\chi_f) \right], \quad (29)$$

which obeys $\Phi_+(0) = \Phi'_+(0) = 0$ by construction. This ansatz leads to a smooth pulse shape $\Omega_+(t)$ that is odd in time, and readily satisfies the initial conditions given in Eq. (23). The coefficients a_i and b_i are free parameters which will be used to find suitable pulse shapes that implement a specific target unitary in the following sections. Furthermore, this form allows enforcing the rotation axis ϕ in Eq. (24) and the desirable property that the microwave source is turned off at the end, $\Omega_+(t_f) = 0$, in an analytical manner:

$$a_1 = \frac{\tan \phi}{\chi_f \sin(2\chi_f)} (1 + \chi_f \cot(2\chi_f) [1 + \sec^2 \phi]), \quad (30)$$

$$a_2 = -\frac{\tan \phi}{3\chi_f^2 \sin(2\chi_f)} (1 + 2\chi_f \cot(2\chi_f) [1 + \sec^2 \phi])$$

Finally, this leads to pulse shapes with modest bandwidth requirements $\Delta f \sim 8/t_f$.

We use the experimentally attainable values of $J = 1\text{MHz}$ and $\delta E_z = 15\text{MHz}$, which yields $\eta \approx 0.0333$ and

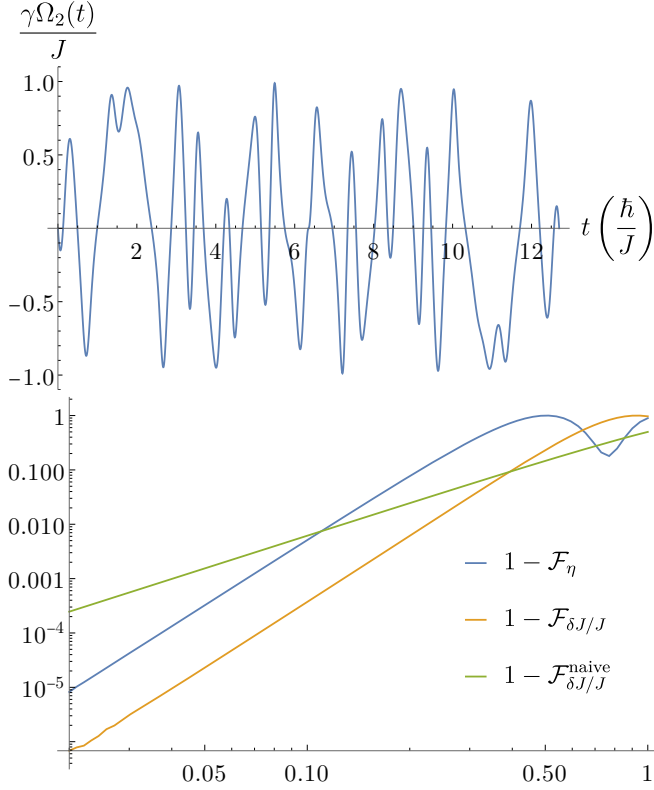


FIG. 1. (Color online) (a) Pulse shape $\gamma\Omega_2(t)$ in units of $J = 1\text{MHz}$ which implements a CZ gate, $\mathcal{R}(\pi/2, 0)$, in $t \approx 13\mu\text{s}$ that is robust against crosstalk ZX term whose strength is characterized by η , and perturbations in exchange δJ . The pulse shape is determined by 8 parameters b_i given in Eq. (32). (b) Infidelity of the robust pulse as a function of perturbation strength, η or $\delta J/J$, compared to the infidelity of a naive pulse with $\Omega_2 = 0$ as a function of $\delta J/J$.

$\gamma \approx 0.9994$. For a given ϕ and θ , we use numerical constrained global optimization to solve for the remaining robustness conditions Eqns. (22a) and (22c), subject to the constraints [35]

$$\max |\gamma\Omega_2(t)| \leq 1\text{MHz}, \quad T \equiv 2t_f \leq 20\mu\text{s}, \quad (31)$$

where T is the total gate time. The first constraint is necessary for improving the accuracy of the Bloch-Siegert shift compensation, where we assumed that $\gamma\Omega_2(t)/\delta E_z$ is a smallness factor whereas the second condition is for keeping the gate time within reasonable limits.

We are only able to find numerical solutions within these constraints if we introduce additional windings to the ZZ rotation as $\theta \rightarrow 2\pi k + \theta$. For a given target angle ϕ , the gate time increases with k , which puts a limit on how small $\Omega_2(t)$ can be; we choose k such that the gate time is minimal.

A. Robust CZ gate

A CZ gate $\exp(-i\frac{\pi}{4}ZZ)$ corresponds to $\theta = \pi/2$ and $\phi = 0$. We take the target angle to be $\theta = 2\pi k + \pi/2$ with $k = 5$, which determines the values of a_i through Eq.(30) as $a_1 = 0$ and $a_2 = 0$, and using numerical optimization for robustness conditions we find

$$\mathbf{b} \approx \{-2.63, 0.07, -0.31, -0.52, 0.09, 0.01, -0.03, -0.06\}. \quad (32)$$

The resulting pulse shape $\Omega_2(t)$, which takes $\approx 12.7\mu\text{s}$ is shown in Fig. 1.

With the ZI Bloch-Siegert correction Eq. (18), the infidelity due to neglecting H_{osc} is $\approx 4 \times 10^{-4}$, whereas using Eq. (19) yield $\approx 9 \times 10^{-5}$. From Fig. 1, we see that an infidelity budget of 10^{-4} is able to tolerate errors up to $\delta J/J \approx 0.075$ (i.e., $\delta J \approx 75\text{kHz}$) and $\eta \approx 0.04$.

Implementing such a smooth pulse shape exactly may be challenging. As an example, we numerically checked that at $\delta J \approx 75\text{kHz}$ exchange error, an imperfect pulse shape with 0.01 errors in all pulse “amplitudes” b_i results in $\approx 3 \times 10^{-4}$ infidelity instead of $\approx 10^{-4}$ with a perfect pulse shape.

We numerically find that the limit on the maximum allowed value of $\gamma\Omega_2$ can be raised to 1.5MHz with similar error characteristics, with a shorter gate time of $T \approx 9.2\mu\text{s}$ at $k = 3$, with parameters

$$\mathbf{b} \approx \{-0.51, 1.62, 0.12, -0.20, 0.05, 0.09, 0.04, -0.01\}. \quad (33)$$

B. Robust one-qubit gates

For implementing one-qubit gates, we make use of the availability of virtual local Z rotations [30–32] as follows. Any one-qubit gate can be expressed in terms of three Euler angles

$$\begin{aligned} IZ_{\alpha_3} IY_{\alpha_2} IZ_{\alpha_1} &= IZ_{\alpha_3} IX_{\frac{\pi}{2}} IZ_{\alpha_2} IX_{-\frac{\pi}{2}} IZ_{\alpha_1} \\ &= -IZ_{\alpha_3} IX_{\frac{\pi}{2}} IZ_{\alpha_2 + \pi} IX_{\frac{\pi}{2}} IZ_{\alpha_1 + \pi}. \end{aligned} \quad (34)$$

This implies that having access to a single robust one-qubit gate, $IX_{\frac{\pi}{2}}$, rather than a set of gates with a continuous parameter, is sufficient.

Such a robust one-qubit gate can be implemented using $\mathcal{R}(\theta, \phi)$ given in Eq. (28), since at $\theta = \pi$ it reduces to the local gate

$$\mathcal{R}(\pi, \phi) = IX_{\phi} ZZ_{\pi} IX_{-\phi} = IX_{2\phi} ZZ_{\pi} = -iIX_{2\phi} IZ_{\pi} ZI_{\pi} \quad (35)$$

The extra IZ and ZI rotations can be cancelled using local virtual Z gates which leaves a pure IX rotation. In the context of Eq. (34), however, this is unnecessary as they combine and cancel to give the relation

$$IZ_{\alpha_3} IY_{\alpha_2} IZ_{\alpha_1} = -IZ_{\alpha_3} \mathcal{R}\left(\pi, \frac{\pi}{4}\right) IZ_{\alpha_2} \mathcal{R}\left(\pi, \frac{\pi}{4}\right) IZ_{\alpha_1}. \quad (36)$$

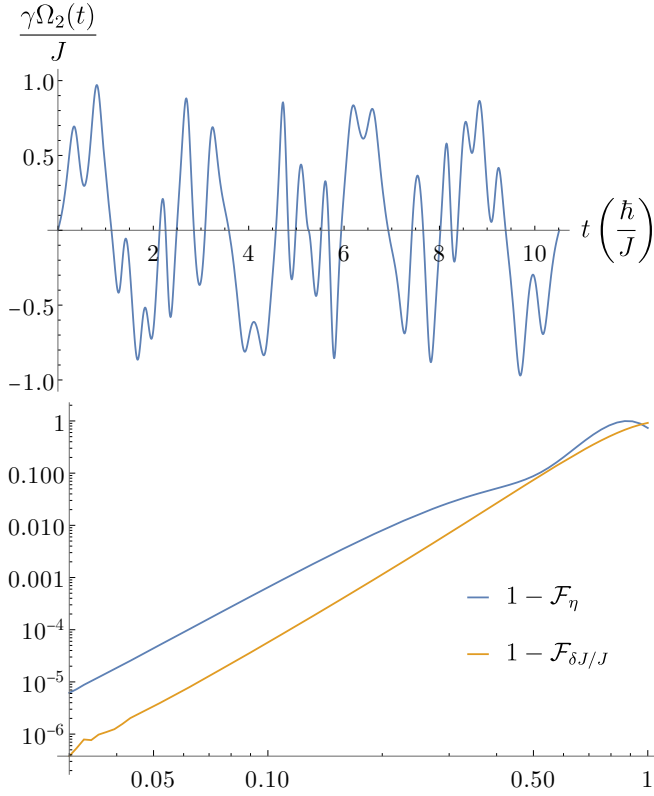


FIG. 2. (Color online) (a) Pulse shape $\gamma\Omega_2(t)$ in units of $J = 1\text{MHz}$ which implements $\mathcal{R}(\pi, \pi/4)$, which is $IX_{\pi/2}$ up to local IZ π -pulses, in $t \approx 11\mu\text{s}$ that is robust against crosstalk ZX term whose strength is characterized by η , and perturbations in exchange δJ . The pulse shape is determined by 8 parameters b_i given in Eq. (37). (b) Infidelity as a function of perturbation strength, η or $\delta J/J$.

We can thus implement any arbitrary one-qubit gate robustly using $\mathcal{R}(\pi, \pi/4)$ in conjunction with virtual IZ rotations.

For finding a pulse shape which implements $\mathcal{R}(\pi, \pi/4)$, we take $\theta = 2\pi k + \pi$ with $k = 4$, and obtain the parameters b_i

$$\mathbf{b} \approx \{-2.52, 0.24, -0.24, -0.48, 0.21, 0.04, 0.02, -0.02\}. \quad (37)$$

The corresponding pulse shape is given in Fig. 2, which takes $\approx 10.5\mu\text{s}$. This implies that arbitrary one-qubit gates can be implemented robustly in $\approx 21\mu\text{s}$.

With the ZI Bloch-Siegert correction from Eq. (18),

the infidelity due to neglecting H_{osc} is $\approx 3 \times 10^{-4}$, whereas using Eq. (19) yield $\approx 2 \times 10^{-4}$. From Fig. 2, we see that an infidelity budget of 10^{-4} allows $\delta J \approx 110\text{kHz}$ and $\eta \approx 0.06$. A perturbation of 0.01 in all b_i results in a loss of fidelity of $\approx 2 \times 10^{-4}$ at $\delta J \approx 110\text{kHz}$. Fig. 2 does not include an infidelity curve for a naive implementation, because one-qubit gates with always-on J coupling is a nontrivial problem even without any robustness requirements [10]. We also observe that at $\delta J \approx 110\text{kHz}$ exchange error, an imperfect pulse shape with 0.01 deviations in all b_i increases the infidelity to $\approx 2 \times 10^{-4}$.

As in the case of CZ gate, we find that raising the limit on the maximum allowed value of $\gamma\Omega_2$ to 1.5MHz yields an $IX_{\pi/2}$ gate with similar error characteristics, and takes $T \approx 8.22\mu\text{s}$ at $k = 3$, with parameters

$$\mathbf{b} \approx \{-0.66, -0.16, -0.22, 0.32, -0.02, 0.03, 0.00, -0.03\}. \quad (38)$$

We note that the gate time for one qubit gates can be improved by making a look up table for \mathbf{b} corresponding to $\mathcal{R}(\pi, \phi)$ for each $2\phi \in [-\pi/2, \pi/2]$, and use instead the ZZZ parametrization for one-qubit rotations as $IZ_{\alpha_3}IX_{\alpha_2}IZ_{\alpha_1}$, which would allow faster implementation of arbitrary one-qubit gates. Such a table with the granularity of $\pi/64$ in ϕ is given in the Appendix A.

VI. CONCLUSION

In summary, we have shown how one can implement a universal set of quantum gates in a silicon double quantum dot setup that is robust against charge noise with always-on exchange coupling and limited addressability. The resulting pulse shapes require a modest bandwidth, and can lead to gates with high fidelity even with systematic errors caused by the signal generator. We expect our results can be implemented in existing devices without modifications.

ACKNOWLEDGMENTS

This research was sponsored by the Army Research Office (ARO), and was accomplished under Grant Number W911NF-17-1-0287.

Appendix A: Parameters for one-qubit gates $X_{2\phi}$

[1] J. Yoneda, K. Takeda, T. Otsuka, T. Nakajima, M. R. Delbecq, G. Allison, T. Honda, T. Kodaera, S. Oda, Y. Hoshi, N. Usami, K. M. Itoh, and S. Tarucha, Nat. Nanotechnol. **13**, 102 (2018).

[2] M. Veldhorst, J. C. C. Hwang, C. H. Yang, A. W. Leenstra, B. de Ronde, J. P. Dehollain, J. T. Muhonen, F. E. Hudson, K. M. Itoh, A. Morello, and A. S. Dzurak, Nat. Nanotechnol. **9**, 981 (2014).

2ϕ	$T(\mu s)$	k	\mathbf{b}
$\frac{\pi}{32}$	14.97	6	$\{-2.52, 0.24, -0.24, -0.48, 0.21, 0.04, 0.02, -0.02\}$
$\frac{2\pi}{32}$	15.05	6	$\{3.06, 0.01, 0.53, 0.45, -0.09, 0.00, -0.09, -0.04\}$
$\frac{3\pi}{32}$	14.97	5	$\{2.60, -0.34, 0.20, 0.35, -0.03, -0.07, -0.06, 0.12\}$
$\frac{4\pi}{32}$	13.02	5	$\{0.12, 1.07, 0.07, 0.03, 0.03, 0.11, -0.04, -0.04\}$
$\frac{5\pi}{32}$	11.86	4	$\{0.79, -0.97, 0.16, 0.13, -0.02, -0.10, -0.05, -0.01\}$
$\frac{6\pi}{32}$	9.92	4	$\{0.72, -0.87, 0.21, 0.17, 0.02, -0.09, -0.02, 0.01\}$
$\frac{7\pi}{32}$	9.90	4	$\{0.56, -0.72, 0.14, 0.14, -0.01, -0.05, 0.00, 0.06\}$
$\frac{8\pi}{32}$	7.89	3	$\{-0.11, 0.78, 0.04, 0.01, 0.05, 0.02, 0.04, 0.03\}$
$\frac{9\pi}{32}$	7.75	3	$\{0.01, 0.61, 0.10, 0.05, 0.06, 0.01, 0.01, 0.01\}$
$\frac{10\pi}{32}$	7.49	3	$\{-0.23, 0.49, -0.02, 0.03, 0.07, 0.06, 0.01, 0.03\}$
$\frac{11\pi}{32}$	7.56	3	$\{-0.26, 0.35, 0.00, -0.03, 0.09, -0.01, 0.03, 0.02\}$
$\frac{12\pi}{32}$	7.57	3	$\{-0.29, 0.21, -0.06, 0.13, 0.08, -0.04, 0.00, 0.01\}$
$\frac{13\pi}{32}$	10.00	4	$\{0.80, 0.27, 0.22, 0.19, 0.00, -0.07, 0.00, 0.03\}$
$\frac{14\pi}{32}$	10.01	4	$\{0.67, 0.30, 0.19, -0.15, -0.01, -0.01, 0.01, 0.02\}$
$\frac{15\pi}{32}$	10.24	4	$\{0.96, 0.47, 0.30, 0.01, 0.01, 0.09, 0.04, 0.04\}$
$\frac{16\pi}{32}$	10.51	4	$\{0.80, 0.30, 0.26, -0.22, -0.07, 0.07, 0.05, 0.03\}$

TABLE I. A look-up table of \mathbf{b} values for implementing a robust $IX_{2\phi}$ gate using k additional 2π rotations in θ , obtained numerically under the constraint that $\gamma\Omega_2(t)$ never exceeds 1MHz. The gate $X_{-2\phi}$ can be implemented with the replacement $a_i, b_i \rightarrow -a_i, -b_i$.

- [3] C. H. Yang, K. W. Chan, R. Harper, W. Huang, T. Evans, J. C. C. Hwang, B. Hensen, A. Laucht, T. Tanttu, F. E. Hudson, S. T. Flammia, K. M. Itoh, A. Morello, S. D. Bartlett, and A. S. Dzurak, Nat. Electron. **2**, 151 (2019).
- [4] S. Lloyd, Phys. Rev. Lett. **75**, 346 (1995).
- [5] R. Brunner, Y.-S. Shin, T. Obata, M. Pioro-Ladrière, T. Kubo, K. Yoshida, T. Taniyama, Y. Tokura, and S. Tarucha, Phys. Rev. Lett. **107**, 146801 (2011).
- [6] M. Veldhorst, C. H. Yang, J. C. C. Hwang, W. Huang, J. P. Dehollain, J. T. Muhonen, S. Simmons, A. Laucht, F. E. Hudson, K. M. Itoh, A. Morello, and A. S. Dzurak, Nature **526**, 410 (2015).
- [7] T. F. Watson, S. G. J. Philips, E. Kawakami, D. R. Ward, P. Scarlino, M. Veldhorst, D. E. Savage, M. G. Lagally, M. Friesen, S. N. Coppersmith, M. A. Eriksson, and L. M. K. Vandersypen, Nature **555**, 633 (2018).
- [8] D. M. Zajac, A. J. Sigillito, M. Russ, F. Borjans, J. M. Taylor, G. Burkard, and J. R. Petta, Science **359**, 439 (2018).
- [9] X. Xue, T. F. Watson, J. Helsen, D. R. Ward, D. E. Savage, M. G. Lagally, S. N. Coppersmith, M. A. Eriksson, S. Wehner, and L. M. K. Vandersypen, Phys. Rev. X **9**, 021011 (2019).
- [10] W. Huang, C. H. Yang, K. W. Chan, T. Tanttu, B. Hensen, R. C. C. Leon, M. A. Fogarty, J. C. C. Hwang, F. E. Hudson, K. M. Itoh, A. Morello, A. Laucht, and A. S. Dzurak, Nature **569**, 532 (2019).
- [11] N. V. Abrosimov, D. G. Aref'ev, P. Becker, H. Bettin, A. D. Bulanov, M. F. Churbanov, S. V. Filimonov, V. A. Gavva, O. N. Godisov, A. V. Gusev, T. V. Kotereva, D. Nietzold, M. Peters, A. M. Potapov, H.-J. Pohl, A. Pramann, H. Riemann, P.-T. Scheel, R. Stosch, S. Wundrack, and S. Zakel, Metrologia **54**, 599 (2017).
- [12] D. Culcer, X. Hu, and S. Das Sarma, Appl. Phys. Lett. **95**, 073102 (2009).
- [13] J. Yoneda, K. Takeda, T. Otsuka, T. Nakajima, M. R. Delbecq, G. Allison, T. Honda, T. Kodera, S. Oda, Y. Hoshi, N. Usami, K. M. Itoh, and S. Tarucha, Nat. Nanotechnol. **13**, 102 (2018).
- [14] U. Güngördü and J. P. Kestner, Phys. Rev. B **99**, 081301(R) (2019).
- [15] R. M. Jock, N. T. Jacobson, P. Harvey-Collard, A. M. Mounce, V. Srinivasa, D. R. Ward, J. Anderson, R. Manginell, J. R. Wendt, M. Rudolph, T. Pluym, J. K. Gamble, A. D. Baczewski, W. M. Witzel, and M. S. Carroll, Nat. Commun. **9**, 1768 (2018).
- [16] K. W. Chan, W. Huang, C. H. Yang, J. C. C. Hwang, B. Hensen, T. Tanttu, F. E. Hudson, K. M. Itoh, A. Laucht, A. Morello, and A. S. Dzurak, Phys. Rev. Appl. **10**, 044017 (2018).
- [17] E. J. Connors, J. Nelson, H. Qiao, L. F. Edge, and J. M. Nichol, arXiv:1907.07549 (2019).
- [18] P. Huang, N. M. Zimmerman, and G. W. Bryant, npj Quantum Inf. **4**, 62 (2018).
- [19] M. Russ, D. M. Zajac, A. J. Sigillito, F. Borjans, J. M. Taylor, J. R. Petta, and G. Burkard, Phys. Rev. B **97**, 085421 (2018).
- [20] F. A. Calderon-Vargas, G. S. Barron, X.-h. Deng, A. J. Sigillito, E. Barnes, and S. E. Economou, Phys. Rev. B **100**, 035304 (2019).
- [21] U. Güngördü and J. P. Kestner, Phys. Rev. B **98**, 165301 (2018).
- [22] R. Ruskov, M. Veldhorst, A. S. Dzurak, and C. Tahan, Phys. Rev. B **98**, 245424 (2018).
- [23] J. C. Hwang, C. H. Yang, M. Veldhorst, N. Hendrickx, M. A. Fogarty, W. Huang, F. E. Hudson, A. Morello, and A. S. Dzurak, Phys. Rev. B **96**, 045302 (2017).
- [24] R. Ferdous, K. W. Chan, M. Veldhorst, J. C. C. Hwang, C. H. Yang, H. Sahasrabudhe, G. Klimeck, A. Morello, A. S. Dzurak, and R. Rahman, Phys. Rev. B **97**, 241401 (2018).

- [25] T. Tanttu, B. Hensen, K. W. Chan, C. H. Yang, W. W. Huang, M. Fogarty, F. Hudson, K. Itoh, D. Culcer, A. Laucht, A. Morello, and A. Dzurak, *Phys. Rev. X* **9**, 021028 (2019).
- [26] E. Barnes, X. Wang, and S. Das Sarma, *Sci. Rep.* **5**, 12685 (2015).
- [27] S. Yang, X. Wang, and S. Das Sarma, *Phys. Rev. B* **83**, 161301 (2011).
- [28] S. Das Sarma, X. Wang, and S. Yang, *Phys. Rev. B* **83**, 235314 (2011).
- [29] T. Meunier, V. E. Calado, and L. M. K. Vandersypen, *Phys. Rev. B* **83**, 121403 (2011).
- [30] D. C. McKay, C. J. Wood, S. Sheldon, J. M. Chow, and J. M. Gambetta, *Phys. Rev. A* **96**, 022330 (2017).
- [31] E. Knill, D. Leibfried, R. Reichle, J. Britton, R. B. Blakestad, J. D. Jost, C. Langer, R. Ozeri, S. Seidelin, and D. J. Wineland, *Phys. Rev. A* **77**, 012307 (2008).
- [32] L. M. K. Vandersypen and I. L. Chuang, *Rev. Mod. Phys.* **76**, 1037 (2005).
- [33] U. Güngördü and J. P. Kestner, *arXiv:1906.12289* (2019).
- [34] The robust pulses also correct for ϵ_2 as well. Such errors through hyperfine interaction would however be negligible for silicon with very low concentration of spinful isotopes, which we consider here.
- [35] We use the Improved Stochastic Ranking Evolution Strategy algorithm implementation in NLOpt and limit the number of iterations to 10^5 . The numerical optimization takes around one minute on an Intel Westmere laptop CPU.